

## A fractal structure in a bouncing ball model\*

Juan Campos, M.J. Romero-Vallés, and Pedro J. Torres<sup>†</sup>*Departamento de Matemática Aplicada, Universidad de Granada, 18071 Granada,  
Spain*

**Abstract.** We analyse new aspects of the dynamics of a model consisting in a bouncing ball falling down a staircase profile with the only action of the gravity. We give numerical evidence of a fractal structure in the parameter space. This complex behaviour is also supported by a bifurcation analysis showing an autosimilar bifurcation scheme.

*AMS Subject Classifications:* 34C28, 34C23

*Keywords:* Impact system; Bouncing; Sliding; Periodic solution; Bifurcation scheme

## 1. Introduction

In the context of dynamical systems, fractals are associated to complex behavior, and it is generally understood that integrable systems can not support fractal structures. Typically, fractals in mechanical systems appear as global attractors of a given Poincaré section (like in the forced pendulum, which is maybe the first example exposed in most of the introductory courses) or as the basin of attraction of a given equilibrium (the well-known “Wada lakes” [7, 9, 11]). Our purpose in this paper is to investigate a fractal structure hidden in an apparently simple impact model already studied in [1]. This fractal appears in the parameter plane as the region of parameters that characterize the existence of a special type of solutions, the so-called *periodic sliding solutions*. The appearance of fractal patterns in parameter spaces is an interesting nonlinear phenomenon already studied in different contexts (see for instance [3, 4, 5, 10]).

---

*E-mail address:* ptorres@ugr.es (P. J. Torres)

\*Supported by D.G.I. MTM2005-03483, Ministerio de Educación y Ciencia, Spain

<sup>†</sup>Corresponding author

The model under consideration consists in a bouncing ball falling down a staircase profile with the only action of gravity, as shown in Fig. 1. If the height and length of the steps are  $a$  and  $b$  respectively, then the motion is ruled by

$$\left. \begin{array}{l} x''(t) = 0 \\ y''(t) = -g, \end{array} \right\} \quad \text{if } y(t) > -aE\left[\frac{x(t)}{b}\right] \quad (1.1)$$

$$y'(t^+) = -ey'(t^-) \quad \text{if } y(t) = -aE\left[\frac{x(t)}{b}\right] \quad (1.2)$$

where  $E[x]$  is the integer part of  $x$  and  $g$  is the gravity constant. System (1.1) models the simple parabolic flight between impacts and (1.2) rules the change of velocity in each partially elastic impact. The number  $e \in (0, 1)$  is the coefficient of restitution. As a whole, we have an impact system that is piecewise integrable. This model is closely related to those studied in [14, 15, 16], which exhibit a regular behavior, and also to the problem of a bouncing ball on an oscillating table [8, 12, 13], where chaotic dynamics appears as a consequence of the external forcing.

As it is pointed out in [1], a trivial rescaling permits to take  $a = b = 1$  without losing generality. Besides, we can fix  $g = 1$  with a time rescaling (or equivalently, an adequate choice of the units of measure). With these considerations, the system is reduced to

$$\left. \begin{array}{l} x''(t) = 0 \\ y''(t) = -1, \end{array} \right\} \quad \text{if } y(t) > -E[x(t)] \quad (1.3)$$

$$y'(t^+) = -ey'(t^-) \quad \text{if } y(t) = -E[x(t)]. \quad (1.4)$$

Note that the horizontal motion of the particle is not affected by the impacts so it is smooth and uniform, that is,  $x(t) = ut + x_0$ , where  $x_0$  is the first component of the initial position and  $u$  is the (constant) horizontal velocity.

One of the most important features of this model is the possibility of an accumulation of impacts. To understand this, let us think in a ball bouncing on a flat ground (which correspond to the limit  $a = 0$  in our model (1.1)-(1.2)). Then, the time between two consecutive impacts follows a geometric law and every solution stops at some finite time  $t_s$ . Now, the usual way to continue the solution is taking  $y(t) \equiv 0$  when  $t > t_s$ . This means that the particle sticks the floor after infinitely many impacts. In the general staircase model, there are solutions that find its stopping time after bouncing infinitely many times on the same step, later, the particle slides until the next border and jumps to the next one with vertical velocity equal to zero. Such solutions are called *sliding solutions*.

In order to describe the geometry of the solutions we will introduce some terminology. Between two consecutive impacts, a solution jumps a given number of steps (maybe zero). Such a number will be refereed as a *jump number*. On the other hand, the number of impacts in a given step is called the *impact number* of this step. The list of jump numbers of a given solution is its *associated word*. Clearly, an accumulation of impacts should be performed in the same step, so its associate word would have an infinite sequence of zeroes. We will collapse this into  $0^\infty$ , and refer to it as an *accumulation tail*. Therefore, sliding solutions are characterized by the presence of

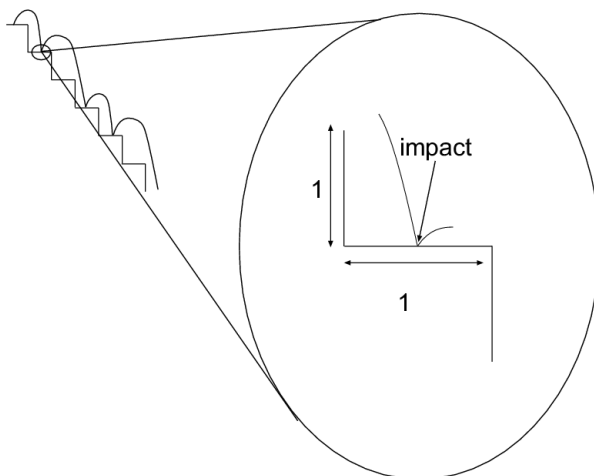


Figure 1: The staircase model

an accumulation tail. Of course, after an accumulation tail there has to be a nonzero jump number. Taking into account the uniform movement in the horizontal variable  $x$ , we will say that a solution is periodic if the height with respect to the stair is periodic, that is, if  $y(t) + E(ut)$  is a periodic function. A periodic solution is described by a finite word. In this paper, we are mainly interested in the periodic solutions of sliding type and more concretely in the description of the region in the parameter plane  $e - u$  where such solutions arise.

The paper is organized as follows. In Section 2 we find the explicit expression of an adequate Poincaré map and use it to give a sufficient condition for non-sliding. This Poincaré map is used in Section 3 to analyze the set of parameters  $(e, u)$  where periodic sliding solutions exist, obtaining a fractal structure that is the center of our work. Finally, Section 4 provides a bifurcation analysis, obtaining for small values of the restitution coefficient  $e$  a regular scheme of discontinuity-induced bifurcations, whereas for  $e$  large a complicated autosimilar bifurcation scheme arises.

## 2. The Poincaré map.

In order to get a better knowledge about the dynamical system we will define a Poincaré map. This will provide us with a good way to build efficient iterative algorithms in the forthcoming sections. Roughly speaking, this Poincaré map measures the relative height and velocity at fixed times  $T = \frac{1}{u}$ , corresponding to the pass of the trajectory over the border of each step (see Fig.2). Mathematically, the Poincaré map  $P : [1, +\infty) \times \mathbb{R} \rightarrow [1, +\infty) \times \mathbb{R}$  is the operator defined as

$$P(y_0, v_0) = (y(T) + 1, y'(T^+)),$$

being  $y(t)$  the corresponding solution of (1.3)-(1.4) that satisfies  $y(0) = y_0, y'(0^+) = v_0$ . The aim of this section is to find the explicit expression of  $P$ . For that, it is necessary to know if the solution slides on a given step or on the contrary there is a finite number of impacts on the step. In order to obtain this information, we will calculate the impact time sequence and investigate its convergence. As a consequence, we will obtain an explicit condition for sliding as well as the exact number of impacts in a given step.

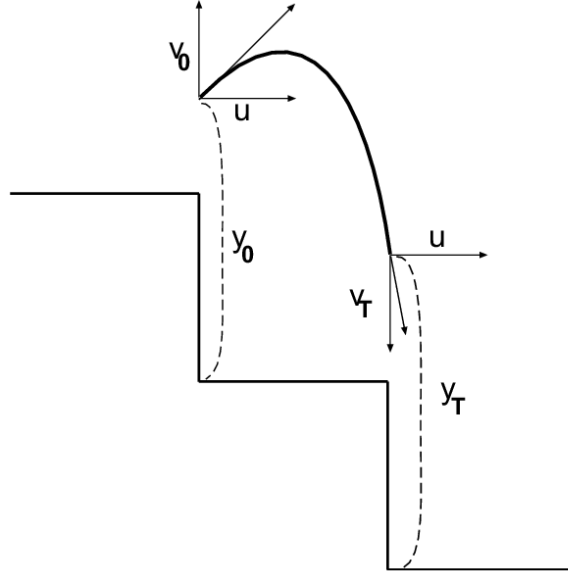


Figure 2: The Poincaré map

For a given  $(y_0, v_0) \in [1, +\infty) \times \mathbb{R}$ , the solution until the first impact is  $y(t) = -\frac{t^2}{2} + v_0 t + y_0$ . If this first impact occurs in the immediate step, the impact time is

$$t_1 = v_0 + \sqrt{v_0^2 + 2y_0},$$

with position and velocity given by

$$\begin{aligned} y_1 &= y(t_1) = 0, \\ v_1 &= y'(t_1^+) = -e(-t_1 + v_0) = e\sqrt{v_0^2 + 2y_0}. \end{aligned} \tag{2.1}$$

Assuming that the subsequent of impacts hold in the same step, such impacts are obtained recursively, taking into account that the solution is  $y(t) = -\frac{(t-t_k)^2}{2} + v_k(t - t_k)$  between two consecutive impacts and  $v_k$  is the velocity after the  $k$ -th impact. Hence,

$$\begin{aligned} t_k &= v_0 + \frac{1+e-2e^k}{1-e} \sqrt{v_0^2 + 2y_0} \\ v_k &= e^k \sqrt{v_0^2 + 2y_0} \end{aligned} \tag{2.2}$$

Using this formula, a sufficient condition for sliding solutions is deduced.

**Proposition 2.1** *Let be  $(y_0, v_0) \in [1, +\infty) \times \mathbb{R}$ . Then, the solution is sliding at the first step if and only if*

$$y_0 \leq \frac{-2e}{(1+e)^2} v_0^2 - \frac{(1-e)^2}{(1+e)^2 u} v_0 + \frac{(1+e)^2}{2u^2(1-e)^2}. \quad (2.3)$$

*Proof.* Let us assume the solution is sliding at the first step. Then, we pass to the limit at the expression for  $t_k$  given by (2.2) and we impose that  $t_\infty = \lim_{k \rightarrow +\infty} t_k$  is less than the period  $T = \frac{1}{u}$ . This gives

$$v_0 + \frac{1+e}{1-e} \sqrt{v_0^2 + 2y_0} \leq \frac{1}{u}. \quad (2.4)$$

In particular,  $\frac{1}{u} - v_0 > 0$  and then

$$\left( \frac{1+e}{1-e} \sqrt{v_0^2 + 2y_0} \right)^2 \leq \left( \frac{1}{u} - v_0 \right)^2, \quad (2.5)$$

which is equivalent to (2.3) after some algebra.

To prove the converse we first note that from (2.3) we obtain (2.5). Taking square roots, we get either (2.4) or

$$\frac{1+e}{1-e} \sqrt{v_0^2 + 2y_0} \leq v_0 - \frac{1}{u} \quad (2.6)$$

but this can not happen since the left hand term is greater than  $|v_0|$ . □

As a consequence of the previous proposition, it is possible to find a region in the parameter space  $e - u$  without sliding solutions.

**Corollary 2.1** *If*

$$u \geq \frac{1-e}{2\sqrt{2e}},$$

*then there are not solutions of sliding type.*

*Proof.* The boundary of the region defined by (2.3) is a parabola. The result is proved by imposing that the value of this vertex is below the straight line  $y_0 = 1$ . By calculation, this vertex is

$$v_0^* = -\frac{(1-e)^2}{4eu}$$

and

$$y_0^* = \frac{(1-e)^2}{8eu^2}.$$

The corollary follows from the condition  $y_0^* \leq 1$ . □

Note that this result improves [1, Theorem 3.2] (after rescaling the gravity to  $g = 1$ , the condition in [1, Theorem 3.2] is  $u \geq \frac{1-e}{2e}$ ). As it is shown in the next section, this condition is optimal in some sense.

**Proposition 2.2** *Let us suppose that the condition (2.3) is not satisfied. Then, for a given initial condition  $(y_0, v_0)$ , the impact number  $k$  is*

$$k = E \left[ \log_e \left( \frac{(v_0 - \frac{1}{u})(1-e)}{2\sqrt{v_0^2 + 2y_0}} + \frac{1+e}{2} \right) \right].$$

*Proof.* Let  $t_k$  be the last impact. Then it must verify that  $t_k \leq T < t_{k+1}$ . So using the formula for the impact time given in (2.2) we get

$$v_0 + \frac{1+e-2e^k}{1-e} \sqrt{v_0^2 + 2y_0} \leq \frac{1}{u} < v_0 + \frac{1+e-2e^{k+1}}{1-e} \sqrt{v_0^2 + 2y_0}$$

Then

$$e^{k+1} < \frac{(v_0 - \frac{1}{u})(1-e)}{2\sqrt{v_0^2 + 2y_0}} + \frac{1+e}{2} \leq e^k$$

and taking logarithms to base  $e$  one gets that  $k$  is the integer part of that logarithm.  $\square$

The argument above allows us to write down the explicit expression of the Poincaré map.

**Proposition 2.3** *The Poincaré map is given by*

$$\begin{aligned} P : [1, +\infty) \times \mathbb{R} &\rightarrow [1, +\infty) \times \mathbb{R} \\ (y_0, v_0) &\rightarrow (y_T, v_T) \end{aligned} \quad (2.7)$$

being

$$\begin{aligned} y_T &= \frac{-(T-t_k)^2}{2} + v_k(T-t_k) + 1 \\ v_T &= -(T-t_k) + v_k \end{aligned}$$

*if the solution does not slide and  $t_k, v_k$  are defined by the last impact. On the other hand, if there is an accumulation of impacts then  $y_T = 1, v_T = 0$ .*

To get a full description of the dynamics of a solution, we only need to iterate the Poincaré map, verifying at each interval  $(jT, (j+1)T)$  the sliding condition (2.3). Besides its theoretical interest, this sliding condition will be used as the stop criterion for the numerical scheme implemented in the next section.

### 3. The fractal structure of the periodic sliding solutions.

The simplest periodic sliding solutions are those of type  $(n, 0^\infty)$ . These solutions jump  $n$  steps and then there is an accumulation of impacts, after which the solution slides until the border and the motion is repeated. Such solutions are characterized in the following theorem.

**Theorem 3.1** *For a given  $n = 1, 2, 3 \dots$ , there are periodic solutions of type  $(n, 0^\infty)$  if and only if*

$$\frac{n-1}{2} < u^2 \leq \frac{n}{2} \left( \frac{1-e}{1+e} \right)^2. \quad (3.1)$$

The proof relies on an explicit study of an equivalent discrete dynamical system, see [1, Pag. 425] for details. In the parameter plane  $e - u$ , the inequalities (3.1) describe some kind of tongues with decreasing area as a function of the jump number  $n$ . We can speak about  $(n, 0^\infty)$ -sliding tongues. It is easy to verify that such tongues finish in the border  $u = \frac{1-e}{2\sqrt{2e}}$  of the exclusion region calculated in Corollary 2.1, so in this sense our computations are sharp. Figure 3 shows the structure of the  $(n, 0^\infty)$ -sliding tongues.

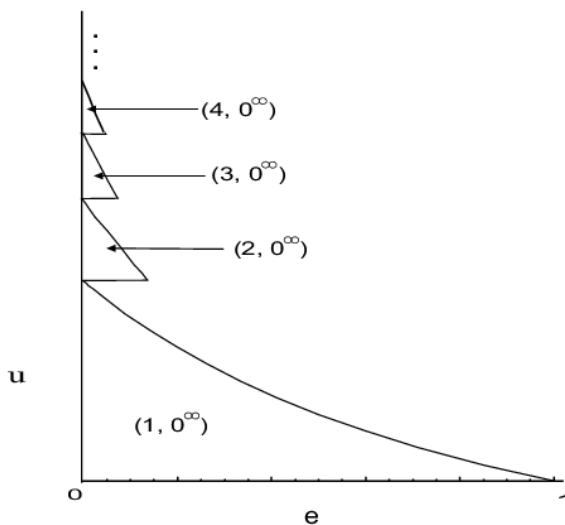


Figure 3: The  $(n, 0^\infty)$ -sliding tongues.

For periodic solutions with more complex associated word, similar explicit arguments become unavailable, but a numerical scheme can be performed. Such numerical scheme works as follows: after a discretization of the given parameter region (we use a fine grid of  $500 \times 350$  points), we compute the successive iterations of the Poincaré map in Section 2 starting with  $(y_0, v_0) = (1, 0)$ . The sliding condition (2.3) is checked in each iteration, working as the stop criterion. Finally, each point of the parameter plane where a sliding solution appears is colored depending on the length of the associated word. The result of this numerical scheme is shown in Figure 4. Note that the black region coincides with Figure 3.

In this graphic and in the following ones, the color indicates the length of the word associated to the corresponding sliding solution. The autosimilarity of this structure is clearly observed if the regions corresponding to consecutive sliding tongues are

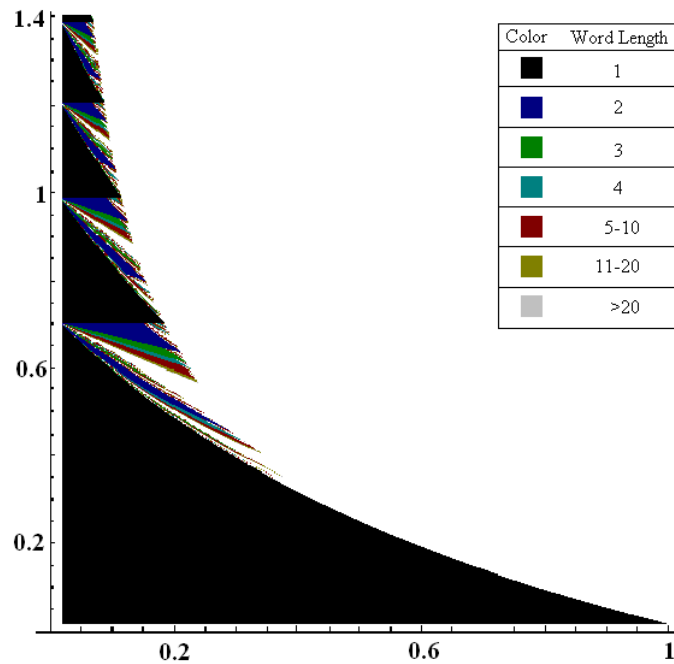


Figure 4: The fractal pattern in the parameter plane  $e - u$ .

enlarged (see Figure 5 a), b) and c)), where it is seen that the same complex structure is repeated at smaller and smaller scales.

The fractal structure of this object is also remarked by enlarging other regions as shown in Fig. 5 d) and e).

The fractal dimension of the perimeter can be numerically computed by a standard box-counting algorithm on the Fig. 6 and 7. The obtained values for the fractal dimension are 1.324 and 1.403 respectively. It is a remarkable fact that these data obtained from the pictures fit the fractal dimension with a correlation coefficient bigger than 0.99.

#### 4. Some bifurcation schemes.

The purpose of this section is to perform a bifurcation analysis for the model under consideration. The strategy is to fix one of the relevant parameters  $e, u$  and move the other one in a certain range. To do that we compute a large number of iterates of an orbit but skipping the first iterates in order to make the diagram independent of the initial condition. This is an usual procedure in the bifurcation analysis of one-dimensional maps, like in the classical period-doubling bifurcation scheme for the logistic equation (see for instance [6]).

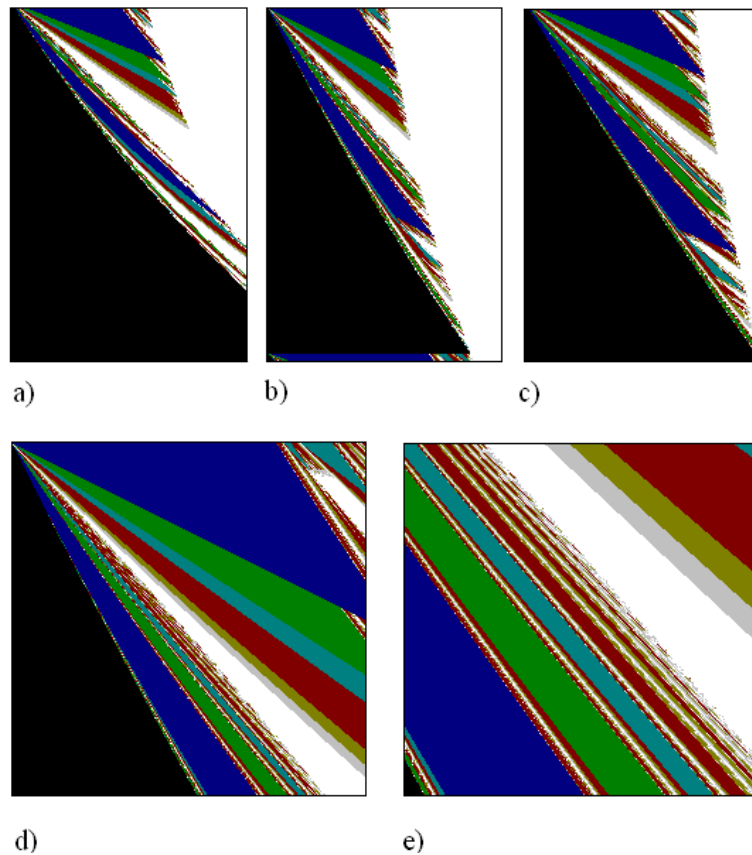


Figure 5: Blowup of a)  $[0, 0.3] \times [0.3, 0.7]$ , b)  $[0, 0.2] \times [0.7, 1]$ , c)  $[0, 0.1] \times [1, 1.22]$ , d)  $[0, 0.1] \times [0.9, 1]$  and e)  $[0.04, 0.065] \times [0.92, 0.945]$ .

We have chosen to fix  $e$  and move  $u$  in a suitable interval partition. Once  $e$  is fixed, for each value of  $u$  the solution is computed starting at  $y_0 = 0.1$  and  $v_0 = 0$  by using the Poincaré map (2.3) obtained in Section 2. We plot the first component of the Poincaré iterates from 2000 to 2200.

We have checked other possibilities (for instance, fix  $u$  and move  $e$ , choose different initial conditions or plot the second component) with similar results.

When  $e$  is small, it is observed a regular bifurcation diagram (see Fig. 8). New branches arise in a regular fashion when the parameter  $u$  enters in a new  $(n, 0^\infty)$ -sliding tongue, corresponding to grazing bifurcations, that is, specific values of  $u$  for which the solution pass just grazing the edge of a step. Such kind of bifurcations are also known as *discontinuity-induced bifurcations* and are common in different classes of non-smooth dynamical systems like some types of electrical circuits described by a piecewise linear system (see [2] and their references).

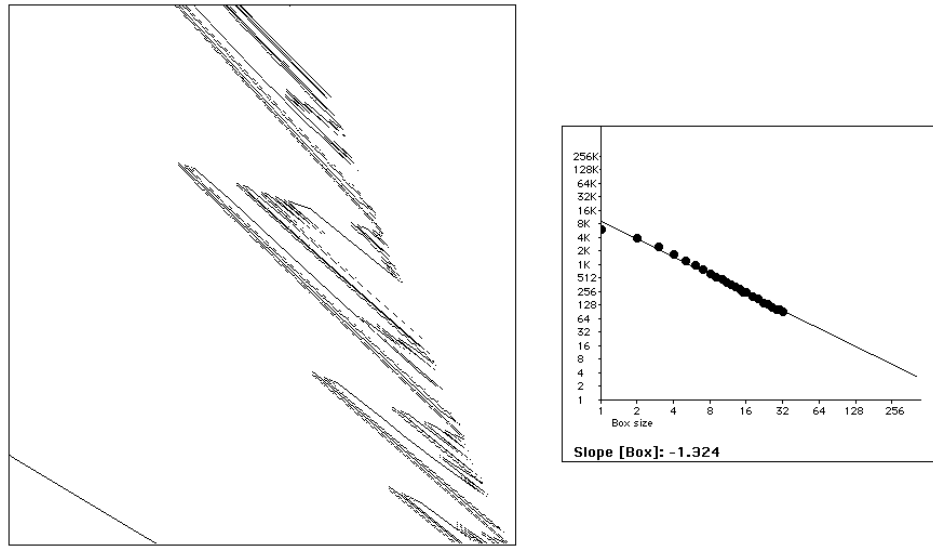


Figure 6: Border of the region  $[0, 0.333] \times [0.4, 0.733]$  and the associated box-counting computation.

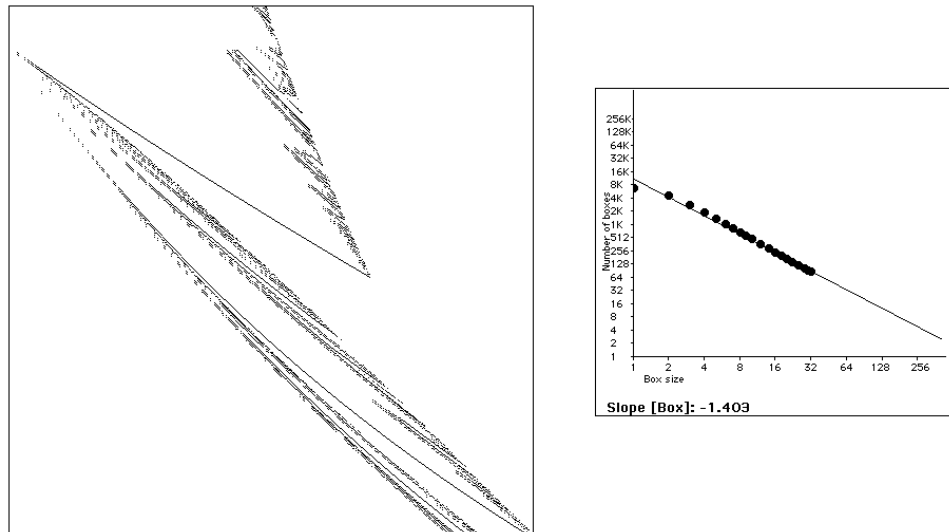
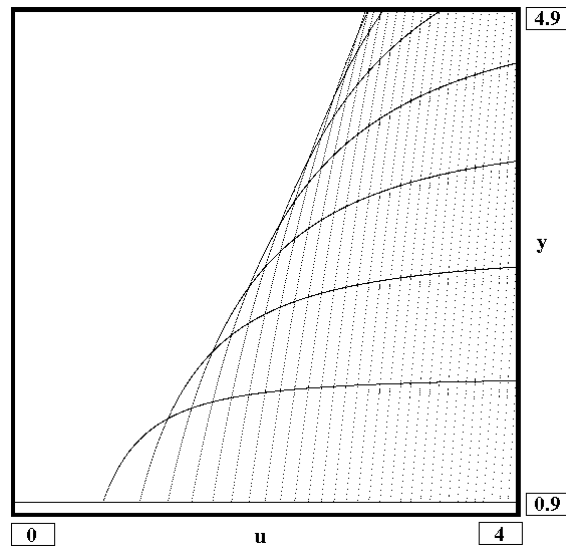
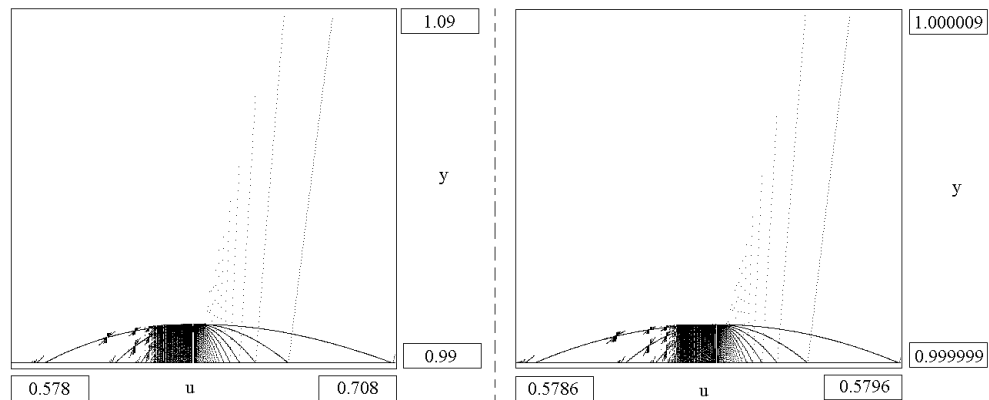


Figure 7: Border of the region  $[0.155, 0.2138] \times [0.6, 0.658]$  and the associated box-counting computation.

Figure 8: Bifurcation diagram for  $e = 0.001$ .

When the coefficient of restitution is higher, for instance  $e = 0.1$ , an autosimilar bifurcation diagram arises by taking the range of  $u$  as a cross-section of the fractal that characterizes the existence of sliding solutions. This complex behavior at smaller and smaller scales is shown in Figure 9.

Figure 9: Bifurcation diagrams for  $e = 0.1$ .

## Acknowledgment

The authors are indebted to an anonymous referee who helped to improve the presentation of the paper in a significant way.

## References

- [1] J. Campos, M.J. Romero, P.J. Torres, J.J.P. Veerman, Dynamics of a jumping particle on a staircase profile, *Chaos, solitons & fractals*, 32:2 (2007), 415–426.
- [2] A. El Aroudi, M. Debbat, R. Giral, G. Olivar, L. Benadero, E. Toribio, Bifurcations in Dc-Dc switching converters: Review of methods and applications, *Int. J. of Bifurcation & Chaos* 15:5 (2005), 1549–1578.
- [3] J. Graczyk, G. Swiatek, Generic hyperbolicity in the logistic family, *Ann. of Math.* 146:1 (1997), 1–52.
- [4] C. Grebogi, S.W. McDonald, E. Ott, J.A. Yorke, Exterior dimension of fat fractals, *Phys. Lett. A* 110:1 (1985), 1–4.
- [5] J.D. Farmer, Sensitive dependence on parameters in nonlinear dynamics, *Phys. Rev. Lett.* 55 (1985), 351–354.
- [6] J. Hale, H. Kocack, “Dynamics and Bifurcations”, Springer, New York, 1991.
- [7] J. Kennedy, J.A. Yorke, Basins of Wada, *Phys. D* 51 (1991), 213–225.
- [8] T.M. Mello, N.B. Tuffillaro, Strange attractors of a bouncing ball, *American J. of Phys.* 55:4 (1987), 316–320.
- [9] H.E. Nusse, J.A. Yorke, Wada basin boundaries and basin cells, *Phys. D* 90:3 (1996), 242–261.
- [10] V. Paar, N. Pavin, Intermingled fractal Arnold tongues, *Phys. Rev. E* 52:2 (1998), 1544–1549.
- [11] S. Takesue, K. Kaneko, Fractal basin structure, *Progr. Theor. Phys.* 71 (1984), 35–49.
- [12] N.B. Tuffillaro, T.M. Mello, Y.M. Choi, A.M. Albano, Period boubling boundaries of a bouncing ball, *Journal de Physique* 47 (1986), 1477–1482.
- [13] N.B. Tuffillaro, A.M. Albano, Chaotic dynamics of a bouncing ball, *American J. of Phys.* 54:10 (1986), 939–944. 47 (1986), 1477.
- [14] J. J. P. Veerman, F. V. Cunha Jr., G. L. Vasconcelos, Dynamics of a granular particle on a rough surface with a staircase profile. VII Latin American Workshop on Nonlinear Phenomena (Morelos, 2001). *Phys. D* 168/169 (2002), 220–234.
- [15] G. L. Vasconcelos, J. J. P. Veerman, Geometrical Models for Grain Dynamics, *Physica A* 271 (1999), 251–259.
- [16] J. J. P. Veerman, A solvable model for gravity driven granular dynamics, *Dynamical Systems* (2005), *Dyn. Sys.* 20:2 (2005), 237–254.